Atmospheric muons and neutrinos

Vadim A. Naumov

Dipartimento di Fisica and Sezione INFN di Ferrara, Via del Paradiso 12, I-44100 Ferrara, Italy and
Laboratory for Theoretical Physics, Irkutsk State University, Gagarin boulevard 20, RU-664003 Irkutsk, Russia

Abstract. This paper is a mini-review of the atmospheric muon and neutrino flux calculations based upon a recent version of CORT code and up-to-date data on primary cosmic rays and hadronic interactions. A comparison of calculations with a representative set of atmospheric muon data for momenta below ~ 1 TeV/c is presented. The overall agreement between the calculated muon fluxes and the data provides an evidence in favor of the validity of adopted description of hadronic interactions and shower development. In particular, this supports the low-energy atmospheric neutrino fluxes predicted with CORT which are essentially lower than those used in current analyses of the sub-GeV and multi-GeV neutrino induced events in underground neutrino detectors.

1 Introduction

In recent paper by Fiorentini *et al.* (2001a) an updated version of FORTRAN code CORT (**C**osmic-**O**rigin **R**adiation **T**ransport) has been described and some results of low and intermediate energy muon and neutrino flux calculations performed with CORT have been discussed. A detailed comparison with the muon fluxes and charge ratios measured in several modern balloon-borne experiments suggests that the atmospheric neutrino flux is essentially lower than one used in the current analyses of the sub-GeV and multi-GeV neutrino induced events in underground detectors. Some additional results which confirm this conclusion were discussed in (Fiorentini *et al.*, 2001b).

Present work can be considered as an *addendum* to the above-mentioned papers. Its main goal is to provide a comparison of the predicted muon fluxes with a more representative set of data from balloon-borne and ground-based experiments, including rather old (but by no means outdated), which cover extensive ranges of muon momenta,[1] zenith angles and atmospheric depths. Such a comparison may be useful to obtain further insight into the atmospheric neutrino problem.

2 The CORT code

Like the earlier versions of CORT (Naumov, 1984; Bugaev and Naumov, 1984, 1985, 1986, 1987a,b, 1988, 1989, 1990; Naumov, 1993; Bugaev *et al.*, 1998), the new Fortran 90 code implements a numerical integration of a system of one-dimensional kinetic equations describing the production and transport of nuclei, nucleons, light mesons, muons, neutrinos, and antineutrinos of low and intermediate energies in the atmosphere. It takes into account solar modulation, geomagnetic and meteorological effects, energy loss of charged particles, muon polarization and depolarization effects. The exact relativistic kinematics is applied for description of particle interactions and decays. The new code has a number of options and run modes. It is rather flexible and permits fast modification of many input data with intrinsic switch keys.

In order to evaluate geomagnetic effects and to take into account the anisotropy of the primary cosmic-ray flux in the vicinity of the Earth, CORT uses the method of Ref. (Naumov, 1984) and detailed maps of the effective vertical cutoff rigidities by Dorman *et al.* (1971). The maps are corrected for the geomagnetic pole drift and compared with the later results reviewed by Smart & Shea (1994) and with the recent AMS data the on the proton flux in near Earth orbit (Alcaraz *et al.*, 2000a). The interpolation between the reference points of the maps is performed by means of two-dimensional local B-spline. The Quenby-Wenk relation (Dorman *et al.*, 1971), re-normalized to the vertical cutoffs, is applied for evaluating

Correspondence to: V. A. Naumov (naumov@fe.infn.it)

[1] In this short write-up we limit ourselves with a selected set of muon data at momenta $p \lesssim 1$ TeV/c (some of these data were taken from the recent compilations by Vulpescu *et al.* (1998, 2001) and Hebbeker & Timmermans (2001)) and do not consider the underground and underwater muon data. Additional data can be found in the comprehensive reference manual by Grieder (2001), and also in Refs. (Bugaev *et al.*, 1998; Naumov, 1998; Naumov *et al.*, 2000a; Sinegovskaya and Sinegovsky, 2001; Naumov, 2001).

the effective cutoffs for oblique directions. More sophisticated effects, like the short-period variations of the geomagnetic field, Forbush decrease, re-entrant cosmic-ray albedo contribution, etc., are neglected. We also neglect the geomagnetic bending of the trajectories of charged secondaries and multiple scattering effects. Validity of our treatment of propagation of secondary nucleons and nuclei has been verified using all available data on secondary proton and neutron spectra in the atmosphere (Naumov, 1984; Bugaev and Naumov, 1984, 1985; Naumov & Sinegovskaya, 2000b, 2001).

The meteorological effects are included using the Dorman model of the atmosphere (Dorman, 1972) which assumes an isothermal stratosphere and constant gradient of temperature (as a function of depths) below the tropopause. Ionization, radiative and photonuclear muon energy losses are treated as continuous processes. This approximation is quite tolerable for atmospheric depths $h \lesssim 2 \times 10^3$ g/cm^2 at all energies of interest (Naumov *et al.*, 1994). Propagation of μ^+ and μ^- originating from every source (pion or kaon decay) is described by separate kinetic equations for muons with definite polarization at production. These equations automatically account for muon depolarization through the energy loss (but not through the Coulomb scattering).

3 Primary cosmic ray spectrum and composition

In the present calculations, the nuclear component of primary cosmic rays is broken up into 5 principal groups: H, He, CNO, Ne-S and Fe with average atomic masses A of 1, 4, 15, 27 and 56, respectively. We do not take into account the isotopic composition of the primary nuclei and assume $Z = A/2$ for $A > 1$, since the expected effect on the secondary lepton fluxes is estimated to be small with respect to present-day experimental uncertainties in the absolute cosmic-ray flux and chemical composition.

We parametrize the spectra of the H and He groups at $E < 120$ GeV/nucleon by fitting the data of the balloon-borne experiment BESS obtained by a flight in 1998 (Sanuki *et al.*, 2000; Sanuki, 2001). For higher energies (but below the knee) we use the data by a series of twelve balloon flights of JACEE (Asakimori *et al.*, 1998) and the result of an analysis by Wiebel-Sooth *et al.* (1998) based upon a representative compilation of world data on primaries. Since the fits obtained by Wiebel-Sooth *et al.* (1998) turned out to be very close to the combined result of the JACEE experiments, the model is called "BESS+JACEE" fit.

Figure 1 shows a comparison between the BESS+JACEE fit, the data from Sanuki *et al.* (2000); Sanuki (2001) (BESS) and Asakimori *et al.* (1998) (JACEE), the fit from Wiebel-Sooth *et al.* (1998) (shaded areas) and the data from several other experiments (Mason, 1972; Ryan *et al.*, 1972; Seo *et al.*, 1991; Beatty *et al.*, 1993; Ichimura *et al.*, 1993; Buckley *et al.*, 1994; Diehl *et al.*, 1997; Menn *et al.*, 2000; Aharonian *et al.*, 1999; Bellotti *et al.*, 1999; Boezio *et al.*, 1999a; Alcaraz *et al.*, 2000b,c), performed in different periods of solar activity. The filled areas in Fig. 1 represent power-type parametrizations of the spectra derived by Asakimori *et al.* (1998); Ryan *et al.* (1972); Ichimura *et al.* (1993); Aharonian *et al.* (1999); Alcaraz *et al.* (2000b,c) from the original data. The legends indicate the publication dates and (when relevant) the years of measurements.

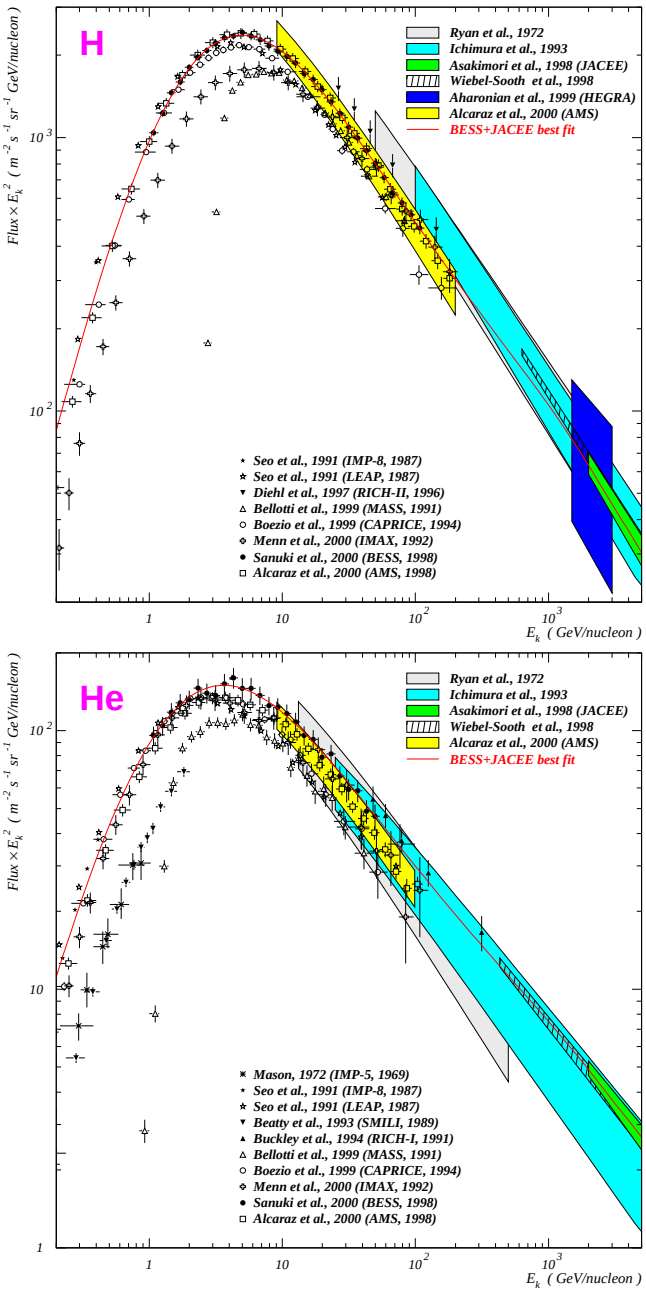

Fig. 1. Differential spectra of protons (top panel) and helium nuclei (bottom panel) as a function of kinetic energy per nucleon. The data points and filled/shaded areas are for the experimental data and power-law fits of the data as is shown in the legends. The solid curves represent the BESS+JACEE best fit from Fiorentini *et al.* (2001a) (see text for details).

We assume that the spectra of the remaining three nuclear groups are similar to the helium spectrum. This assumption does not contradict the world data for the CNO and Ne-

S nuclear groups but works a bit worse for the iron group. Nevertheless, a more sophisticated model would be unpractical since the corresponding correction would affect the secondary lepton fluxes by a negligible margin.

In this paper we do not consider the effects of solar modulation. Therefore the predicted muon and neutrino fluxes are to some extent the maximum ones possible within our approach.

4 Nucleon-nucleus and nucleus-nucleus interactions

All calculations with the earlier version of CORT were based on semiempirical models for inclusive nucleon and meson production in collisions of nucleons with nuclei by Kimel' & Mokhov (1974, 1975); Serov & Sychev (1973).[2] The Kimel'-Mokhov (KM) model is valid for projectile nucleon momenta above ~ 4 GeV/c and for the secondary nucleon, pion and kaon momenta above 450, 150 and 300 MeV/c, respectively. Outside these ranges (that is mainly within the region of resonance production of pions) the Serov-Sychev (SS) model was used.

Both models are in essence comprehensive parametrizations of the relevant accelerator data. It is believed that the combined "KM+SS" model provides a safe and model-independent basis to the low-energy atmospheric muon and neutrino calculations. However it is not free of uncertainties. For the present calculation, the fitting parameters of the KM model for meson and nucleon production off different nuclear targets were updated using accelerator data not available for the original analysis (Kimel' & Mokhov, 1974, 1975; Kalinovsky *et al.*, 1985). The values of the parameters were extrapolated to the air nuclei (N, O, Ar, C). The overall correction is less than 10-15% within the kinematic regions significant to atmospheric cascade calculations. Besides that energy-dependent correction factors were introduced into the model to tune up the output π^+/π^- ratio taking into account the relevant new data.

The processes of meson regeneration and charge exchange ($\pi^\pm + \mathrm{Air} \to \pi^{\pm(\mp)} + X$ etc.) are not of critical importance for production of leptons with energies of our interest and can be considered in a simplified way. Here we use a proper renormalization of the meson interaction lengths, which was deduced from the results by Vall *et al.* (1986) obtained for high-energy cascades.

The next important ingredient of any cascade calculations is a model for nucleus-nucleus collisions. Here we consider a modest generalization of a simple "Glauber-like" model used in (Naumov, 1984; Bugaev and Naumov, 1985). Namely, we write the inclusive spectrum of secondary particles c ($c = p$, n, $\pi^\pm$, $K^\pm$, $K^0, \dots$) produced in collisions of nuclei as

$$\frac{dN_{\mathrm{AB}\to cX}}{dx} = \xi^c_{\mathrm{AB}} \left[Z \frac{dN_{p\mathrm{B}\to cX}}{dx} + (A-Z) \frac{dN_{n\mathrm{B}\to cX}}{dx} \right] + (1-\xi^c_{\mathrm{AB}}) \left[Z\delta_{cp} + (A-Z)\delta_{cn} \right] \delta(1-x).$$

Here $dN_{N\mathrm{B}\to cX}/dx$ is the spectrum of particles c produced in a collision of a nucleon N ($N = p, n$) with nucleus B, x is the Feynman variable, and ξ^c_{AB} is the average fraction of inelastically interacting nucleons of the projectile nucleus A. The term proportional to delta function describes the contribution of "spectator" nucleons from the projectile nucleus.

In the standard Glauber-Gribov multiple scattering theory the quantity ξ^c_{AB} is certainly independent of the type of inclusive particle c. On the other hand, it depends of the type of nucleus collision. Indeed, essentially all nucleons participate in the central AB collisions ($\xi^c_{\mathrm{AB}} \simeq 1$)[3] while, according to the well-known Bialas–Bleszyński–Czyż (BBC) relation (Bialas *et al.*, 1976), $\xi^c_{\mathrm{AB}} = \sigma^{\mathrm{inel}}_{N\mathrm{B}}/\sigma^{\mathrm{inel}}_{\mathrm{AB}}$ for the minimum bias collisions.

To use the above model in a cascade calculation one should take into account that nucleons and mesons are effectively produced in nuclear collisions of different kind. Namely, the contribution from central collisions is almost inessential for the nucleon component of the cascade but quite important for light meson production. Thus one can expect that effectively $\xi^{\pi,K}_{\mathrm{AB}} > \xi^{p,n}_{\mathrm{AB}}$. We use the BBC relation for nucleon production by any nucleus while for meson production we put $\xi^{\pi,K}_{\mathrm{He-Air}} = \xi$, where ξ is a free parameter. Variations of this parameter within the experimental limits yield a comparatively small effect to the muon fluxes (except for very high altitudes) and inessential ($\lesssim 6\%$) effect to the neutrino fluxes at sea level (Fiorentini *et al.*, 2001a). Effect of similar variations of the parameters $\xi^{\pi,K}_{\mathrm{A-Air}}$ for other nuclear groups is completely negligible.

5 Numerical results for muons

Figure 2 displays a comparison of the calculated momentum spectra of μ^+ and μ^- for 10 atmospheric depth ranges $\Delta h_i = 15-35, 35-65, 65-90, 90-120, 120-150, 150-190, 190-250, 250-380, 380-580$, and $580-890$ g/cm^2 with the data of two balloon-borne experiments CAPRICE 94 (Boezio *et al.*, 1999, 2000) and CAPRICE 98 (Hansen *et al.*, 2001) (the latter experimental data are *preliminary*). The nominal geomagnetic cutoff rigidity R_c is about 0.5 GV (4.5 GV) and the detection cone is about 20° (14°) around the vertical direction with the average incident angle of about 9° (8°) for CAPRICE 94 (CAPRICE 98). The data points in Fig. 2 are the muon intensities at the Flux-weighted Average Depths (FAD) defined in (Boezio *et al.*, 1999), while the filled areas display the calculated variations of the muon spectra inside the ranges Δh_i ($i = 1, \dots, 10$). Namely, they are obtained by considering the minimal and maximal muon fluxes within each range Δh_i. The calculations are performed for the conditions of the experiment. The parameter ξ is taken to be 0.685 (the best value, according to Fiorentini *et al.* (2001a)).[4]

[2] See also Refs. Kalinovsky *et al.* (1985); Sychev (1999) for the most recent versions.

[3] Here we assume for simplicity that the atomic weight of the projectile nucleus is not much larger than that of the target nucleus.

[4] It has been shown (Fiorentini *et al.*, 2001a) that the indetermination of ξ is only significant for $h < (15-20)$ g/cm^2.

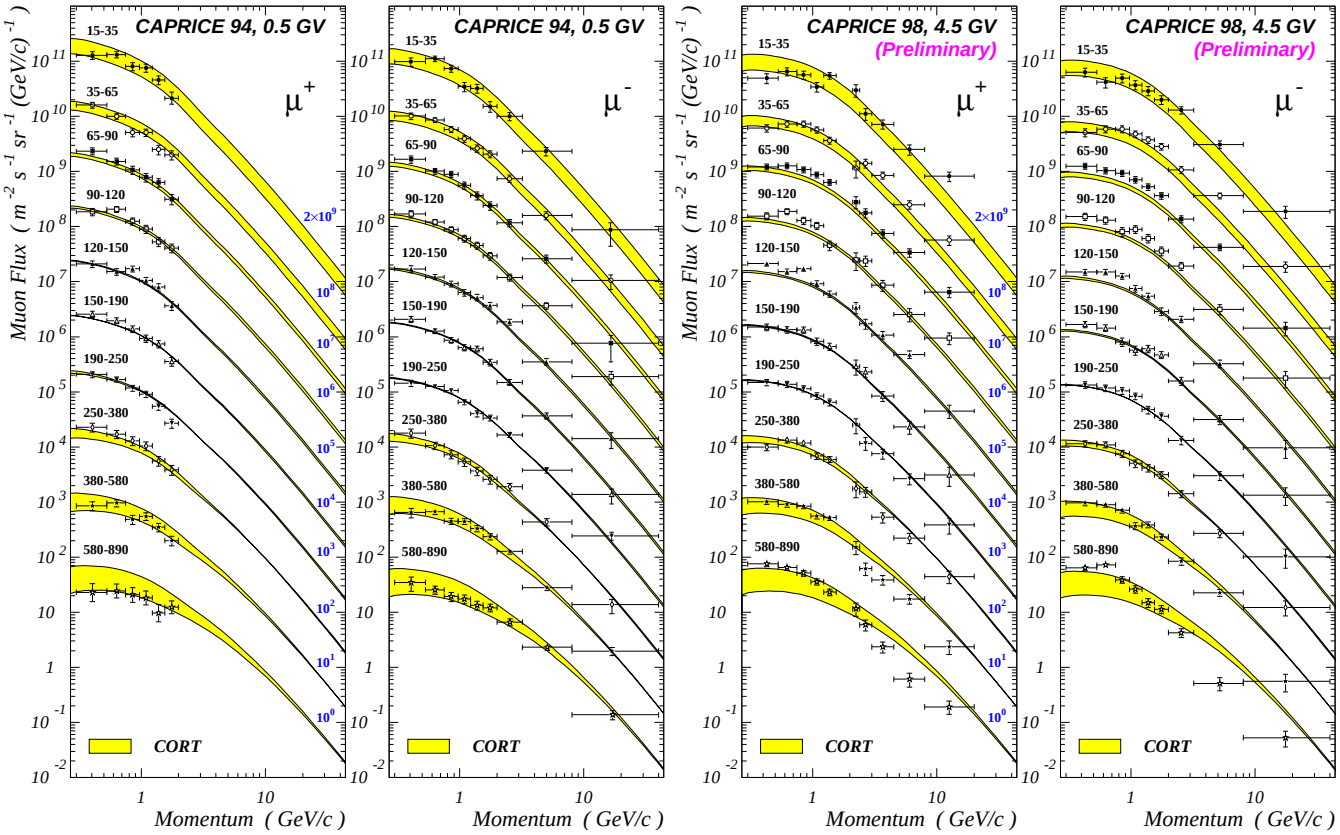

Fig. 2. Differential momentum spectra of μ^+ and μ^- for 10 atmospheric depth ranges Δh_i (are indicated on the left of each panel). The data points are from the CAPRICE 94 experiment (Boezio *et al.*, 1999, 2000) and from the *preliminary* analysis of the CAPRICE 98 experiment (Hansen *et al.*, 2001). The filled areas display the expected variations of the muon fluxes within the ranges Δh_i. All the data are scaled with the factors indicated at the first and third panels on the right.

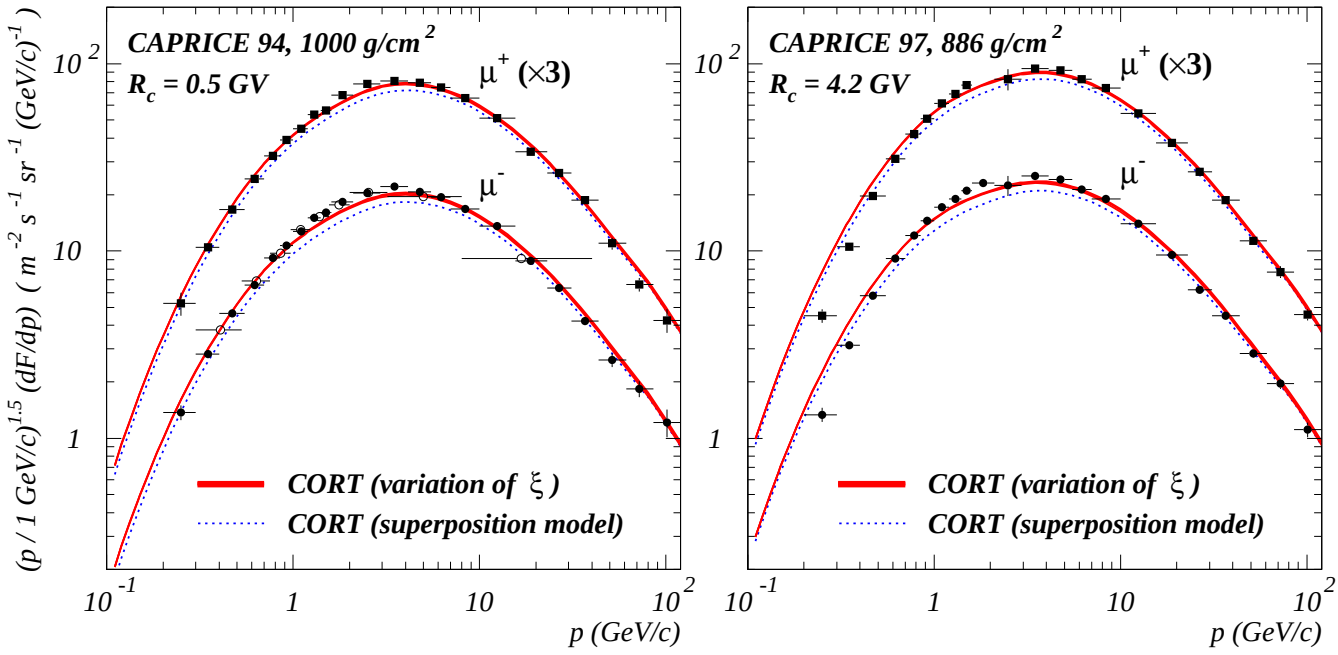

Fig. 3. Differential momentum spectra of positive and negative muons at the ground level. The data points are from the experiments CAPRICE 94 (Boezio *et al.*, 1999, 2000; Kremer *et al.*, 1999) and CAPRICE 97 (Kremer *et al.*, 1999). The μ^+ data are scaled with a factor of 3. The solid (narrow) bands and dotted curves are calculated with CORT as is explained in legends.

It is important to note that the thickness of the bands is relatively small just for the region of effective muon and neutrino production that is in the neighborhood of the broad maxima of the muon flux ($100-300$ g/cm^2). By this is meant that, in this region, an error in evaluation of the FAD cannot introduce essential uncertainty. Outside the region of effective production of leptons, the amplitude of the muon flux variations increases with decreasing muon momenta on account for the strong dependence of the meson production rate upon the depth and the growing role of the muon energy loss and decay at $h \gtrsim 300$ g/cm^2.

Figure 3 shows a comparison of the calculated differential momentum spectra of μ^+ and μ^- with the most accurate current data obtained at ground level in the experiments CAPRICE 94 (Boezio *et al.*, 1999, 2000; Kremer *et al.*, 1999) ($h = 1000$ g/cm^2, $R_c = 0.5$ GV) and CAPRICE 97 (Kremer *et al.*, 1999) ($h = 886$ g/cm^2, $R_c = 4.2$ GV). The detection cone in both experiments was the same as described above for CAPRICE 94. The calculation are done by using the KM+SS interaction model. Variation of the parameter ξ from 0.517 (the BBC value) to 0.710 (an experimental upper limit derived from the data on interactions of α particles with light nuclei).[5] leads to the almost negligible ($\lesssim 3\%$) effect in the ground-level muon flux. For reference, the spectra calculated by using the superposition model for nucleus-nucleus interactions are also added. The data below ~ 10 GeV/c seem to be precise enough in order to conclude that they disfavor the superposition model.

As is seen from Figs. 2 and 3, there is a substantial agreement between the calculations with CORT and the data of the CAPRICE experiments within a wide range atmospheric depths. This agreement is *none the worse* than it is for the recent 3D Monte Carlo calculations (Battistoni *et al.*, 2001a; Engel *et al.*, 2001; Honda *et al.*, 2001b; Liu *et al.*, 2001; Poirier *et al.*, 2001; Wentz *et al.*, 2001a,b).[6]

Figure 4 shows expected geomagnetic effect for vertical differential momentum spectra of μ^+ and μ^- and for muon charge ratio μ^+/μ^- at sea level. A comparison of these predictions with experiment will be discussed elsewhere.

Figure 5 collects the data on the near-vertical differential momentum spectrum of $\mu^+ + \mu^-$ at ground level from many experiments performed over the past five decades (Caro *et al.*, 1950; Owen & Wilson, 1955; Pine *et al.*, 1959; Pak *et al.*, 1961; Holmes *et al.*, 1961; Hayman & Wolfendale, 1962a,b; Aurela & Wolfendale, 1967; Baber *et al.*, 1968a; Allkofer & Clausen, 1970; Allkofer *et al.*, 1970, 1971; Bateman *et al.*, 1971; Nandi & Sinha, 1972a; Allkofer *et al.*, 1975; Ayre *et al.*, 1975; Thompson *et al.*, 1977; Baschiera *et al.*, 1979; Green *et al.*, 1979; Rastin, 1984a; Tsuji *et al.*, 1998; Kremer *et al.*, 1999; Le Coultre, 2001). Only the data for muon momenta below ~ 1 TeV/c are shown.

The compilation, of course, is not exhaustive. In particular, it does not involve the low-energy data for large geomagnetic cutoffs, the ground-level data obtained at the altitudes far different from sea level, and also indirect muon data from underground measurements.[7] The spectra calculated for $h = 10^3$ g/cm^2, $\theta = 0^\circ$, and $R_c = 0$ with the new and old (from Bugaev *et al.* (1998)) versions of CORT are plotted. The best-fit spectrum to Nottingham data (Rastin, 1984a) and the spectrum calculated by Agrawal *et al.* (1996) are also shown in bottom panel.

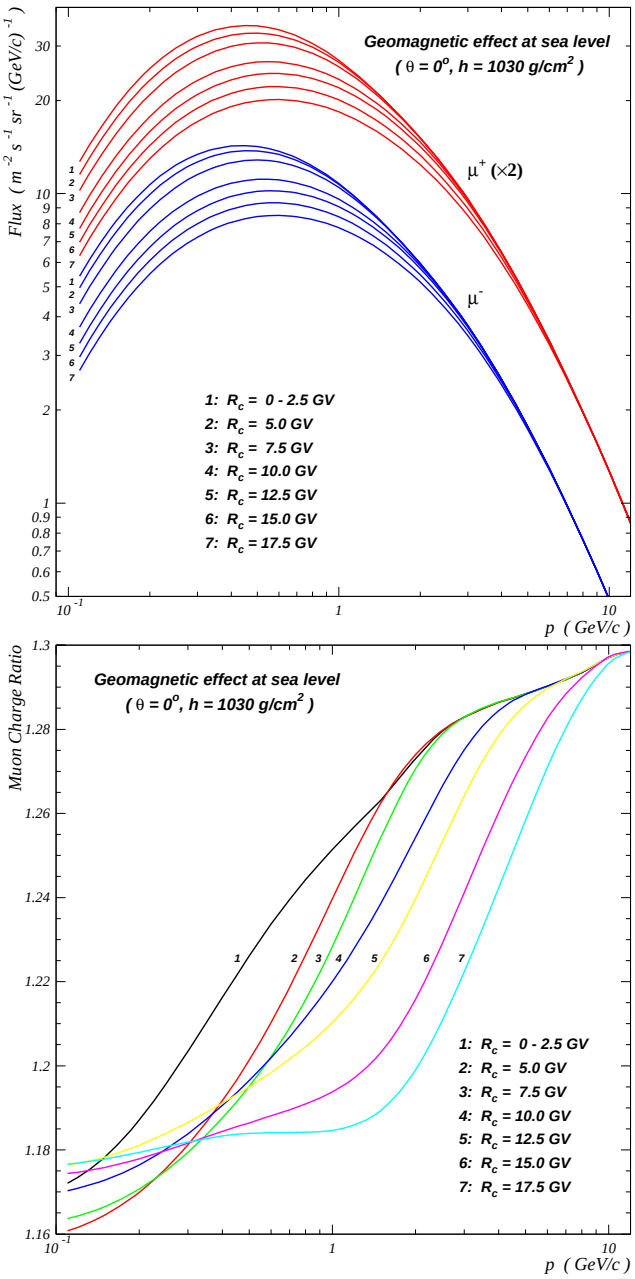

Fig. 4. Vertical differential momentum spectra of positive and negative muons and muon charge ratios at sea level calculated with CORT for several geomagnetic cutoffs R_c. The μ^+ spectra on the top panel are scaled with a factor of 2.

[5] See, e.g., Ref. (Kowalski & Bartke, 1981) and references therein.

[6] See also Ref. (Fiorentini *et al.*, 2001b) for the direct comparison with the FLUKA 3D result.

[7] These were discussed in detail by Bugaev *et al.* (1998).

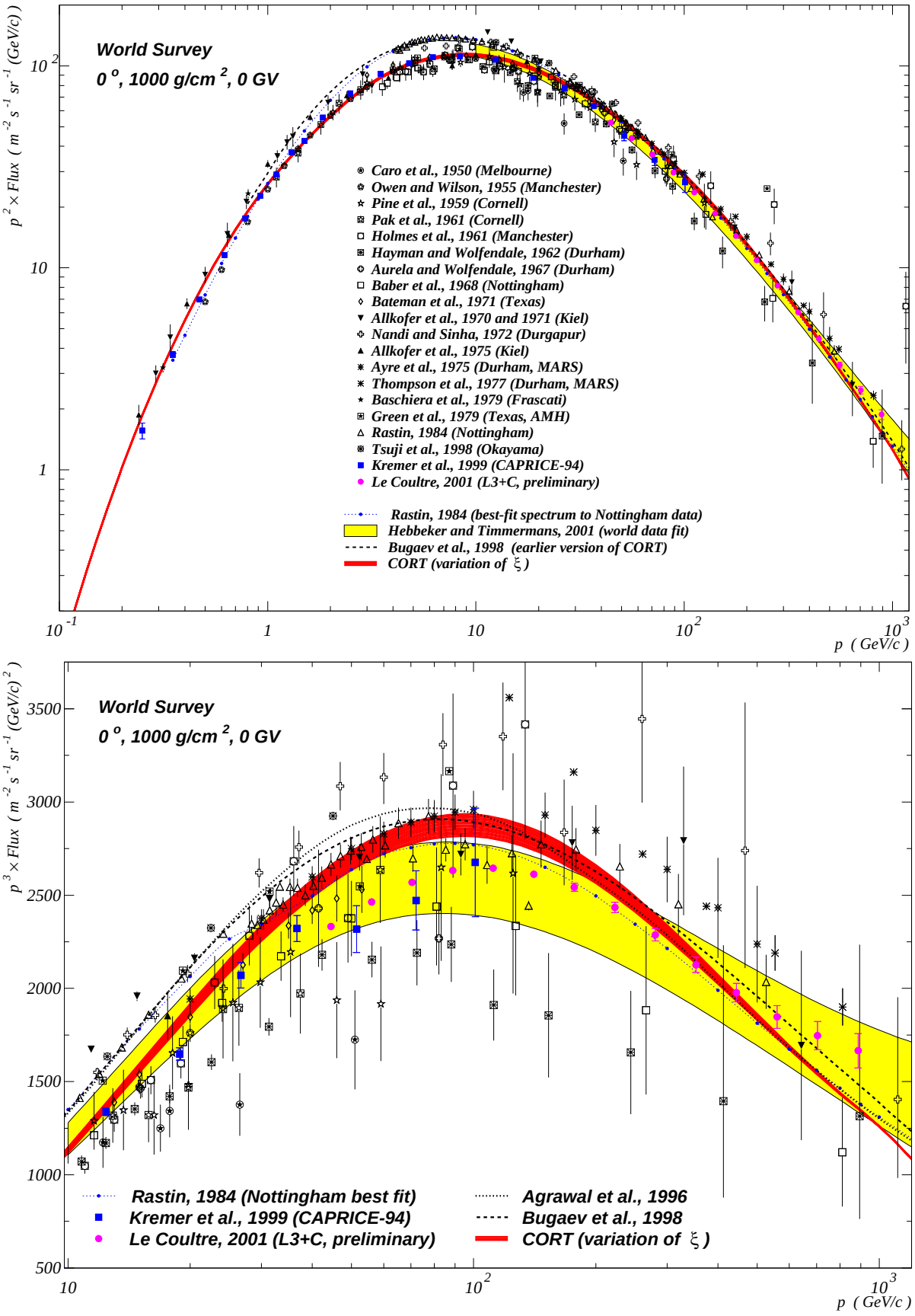

Fig. 5. Near-vertical differential momentum spectrum of $\mu^+ + \mu^-$ at ground level (top panel) and its rescaled fragment for $p > 10$ GeV/c (bottom panel). The thickness of the band calculated with CORT reflects the indetermination in the parameter ξ.

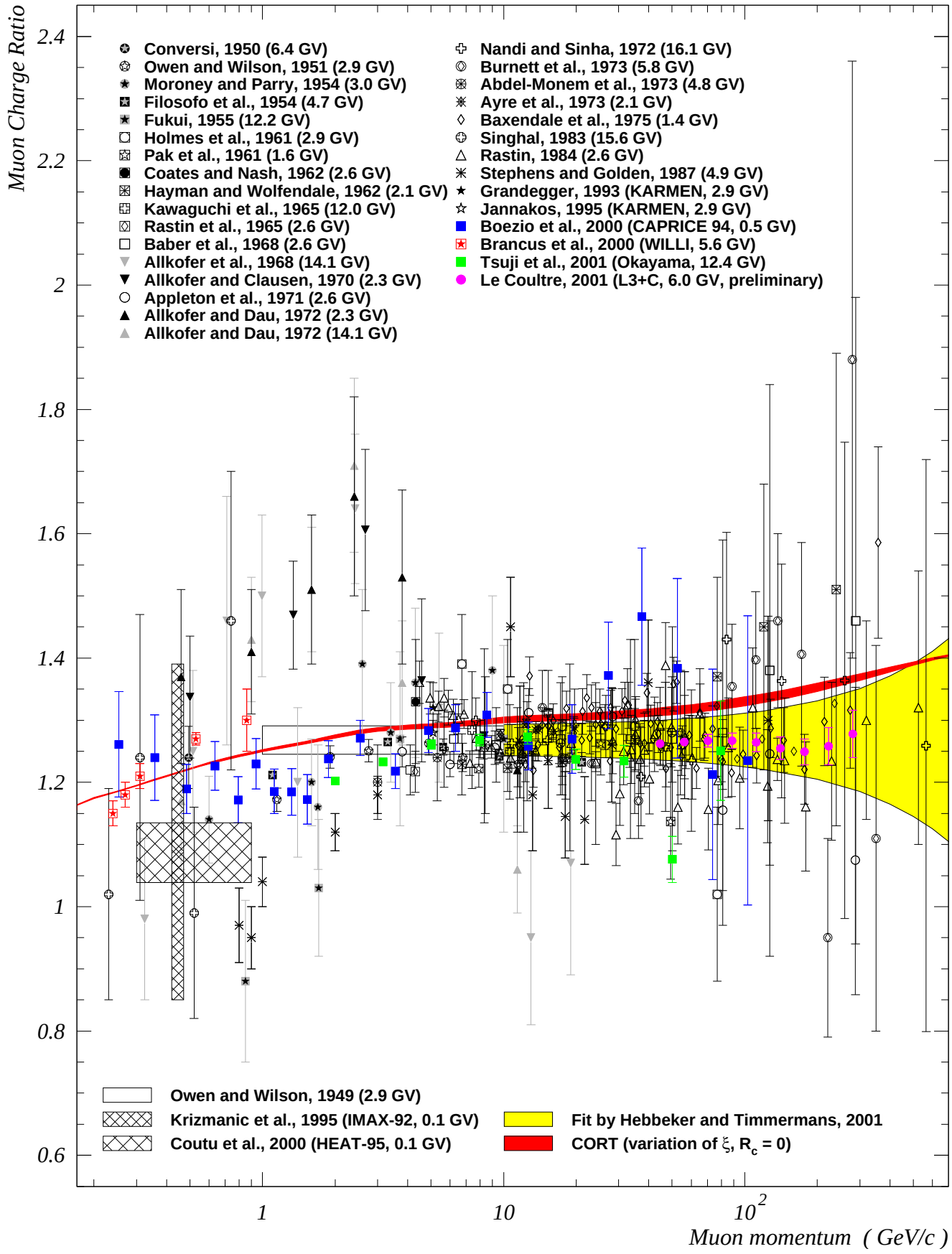

Fig. 6. Muon charge ratio at sea level for near-vertical direction. Geomagnetic cutoffs R_c for different experiments are shown in the legend.

In fact, not all experiments listed above measure at sea level. Moreover, the experiments were performed in different locations and periods. Therefore the solar modulation effects, meteorological and geomagnetic conditions are generally different in these experiments. The same is true for the detection cones, shielding factors, adopted procedures for the momentum spectrum unfolding, and so on. All these factors might cause a bias when all the data are compared together (Hebbeker & Timmermans, 2001). Here we do not pursue any correction procedure (like one suggested by Hebbeker & Timmermans (2001)) and plot all the experimental data as they are. Instead we show the world average fit derived by Hebbeker & Timmermans (2001) from an analysis of (almost) the same data set at $p \geq 10$ GeV/c. It can be seen that the ground-level experiments are in rather poor agreement to one another. A large share of the data are arranged outside (or even far from) the borderline of the world average fit. However the data of the most recent experiments, specifically CAPRICE 94 (Kremer *et al.*, 1999) and L3+C (Le Coultre, 2001) are placed close to or within these bounds.[8]

Fig. 5 suggests that the muon flux calculated with the new CORT is systematically lower than that obtained by Bugaev *et al.* (1998) using the earlier version. The deviation is about 18% for $p = 10$ GeV/c and about a few per cent for $p \gtrsim 80$ GeV/c. The main reason of this difference is that the BESS+JACEE primary spectrum below ~ 200 GeV/nucleon is essentially lower than that used by Bugaev *et al.* (1998) and in the earlier calculations with CORT. Another reasons pertain to the changes in the inclusive cross sections and improved description of muon propagation. Below ~ 400 GeV/c the new spectrum is close to the world average fit and to the data from CAPRICE 94 and L3+C experiments as well as to the data from several experiments carried out by the BESS Collaboration (Sanuki, 2001; Motoki *et al.*, 2001; Sanuki *et al.*, 2001).[9]

Let us now dwell to the muon charge ratio. It has been shown (Fiorentini *et al.*, 2001a) that calculations with CORT describe well the modern data on the charge ratio obtained at different atmospheric depths. Here we consider only the ground-level data for near-vertical directions. The world survey is presented in Fig. 6. The data are taken from many experiments (Owen & Wilson, 1949; Conversi, 1950; Owen & Wilson, 1951; Moroney & Parry, 1954; Filosofo, 1954; Fukui, 1955; Holmes *et al.*, 1961; Pak *et al.*, 1961; Coates & Nash, 1962; Hayman & Wolfendale, 1962a,b; Kawaguchi *et al.*, 1965; Rastin *et al.*, 1965; Baber *et al.*, 1968b; Allkofer *et al.*, 1968; Allkofer & Clausen, 1970; Appleton *et al.*, 1971; Allkofer & Dau, 1972; Nandi & Sinha, 1972b; Burnett *et al.*, 1973; Abdel-Monem *et al.*, 1973; Ayre *et al.*, 1973; Baxendale *et al.*, 1975; Singhal, 1983; Rastin, 1984b; Stephens & Golden, 1987; Grandegger, 1993; Jannakos, 1995; Krizmanic *et al.*, 1995; Boezio *et al.*, 2000; Coutu *et al.*, 2000; Brancus *et al.*, 2000; Tsuji *et al.*, 2001; Le Coultre, 2001), performed at different geomagnetic locations. According to CORT (see bottom panel of Fig. 4), the sea-level charge ratio is slightly affected by the geomagnetic field. However the dispersion of the experimental points is too large and they do not show some significant correlation with the geomagnetic cutoff.

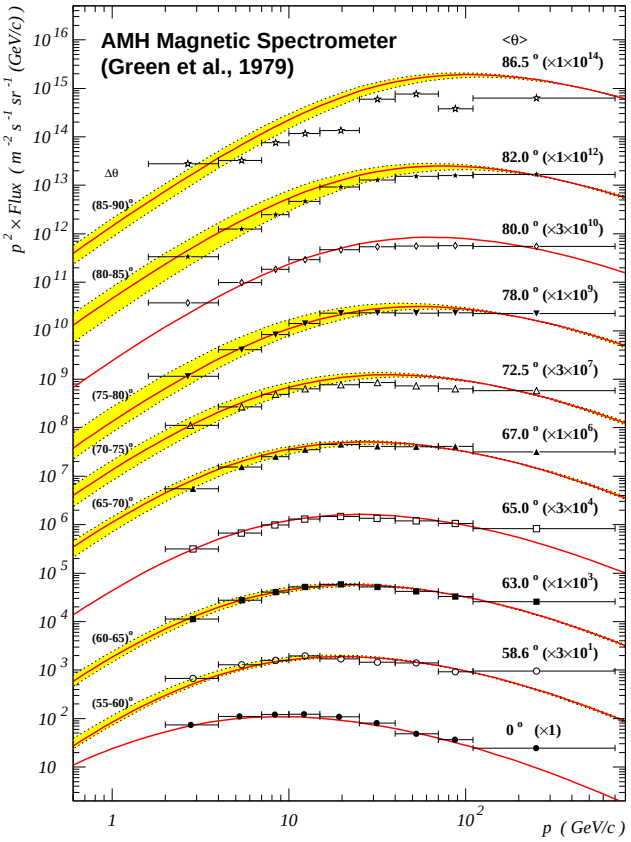

Fig. 7. Differential momentum spectra of muons at sea level for several zenith angles and angular bins. The data points are from AMH spectrometer (Green *et al.*, 1979). The filled areas display the expected variations of the muon fluxes inside the bins $\Delta\theta$ indicated at the left. The solid curves are calculated for average zenith angles $\langle\theta\rangle$. All the data are scaled with the factors shown in the parentheses at the right.

Figure 7 shows a comparison with the sea-level data from the AMH magnetic spectrometer (Texas A & M and University of Houston Collaboration) measured within different zenith-angle bins $\Delta\theta$ (Green *et al.*, 1979). The spectra for average zenith angles and expected variations of the spectra inside the angular bins are shown by solid lines and filed areas, respectively. One can see a good or at least qualitative agreement with the data for $p \lesssim 100$ GeV/c and $\theta \lesssim 80°$. At higher momenta and at large zenith angles the situation is spoiled. However, a comparison between the AMH and world survey data for vertical (see Fig. 5) suggests that there

[8] Note that the L3+C data on muon flux and charge ratio reported in ICRC'27 (Le Coultre, 2001) (see also Refs. (Petersen, 2001; Ladron de Guevara, 2001)), are preliminary and may be subject to refinement (within the systematic error of 7.7%) when analyses are complete.

[9] Unfortunately, the tabulated muon data are still unavailable from the BESS Collaboration.

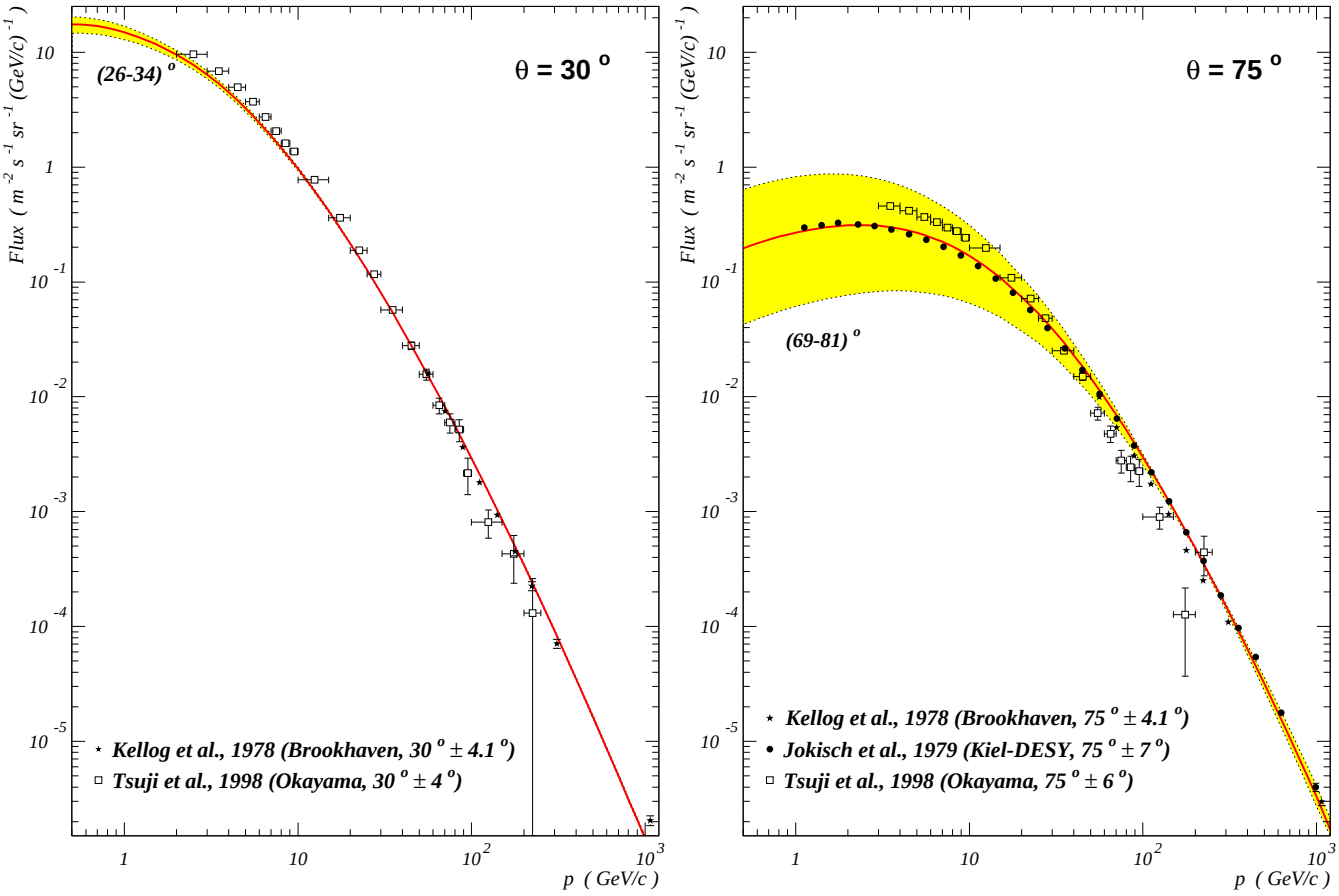

Fig. 8. Differential momentum spectra of muons at sea level for $\theta = 30^\circ$ and 75°. The data points are from (Kellogg *et al.*, 1978; Jokisch *et al.*, 1979; Tsuji *et al.*, 1998). The filled areas display expected variations of the muon fluxes inside the indicated angular bins. The solid curves are for the corresponding average zenith angles.

is some systematic bias in the AMH experiment above 100 GeV/c. The abnormal scatter of points in the near-horizontal bin is indicative of a flaw in the large-angle measurements.

Figure 8 displays a comparison between the differential momentum spectra of muons at ground level calculated with CORT and the data from Brookhaven magnetic spectrometer (Kellogg *et al.*, 1978), Kiel-DESY muon spectrometer located at Hamburg (Jokisch *et al.*, 1979), and Okayama altazimuthal counter cosmic-ray telescope with a magnet spectrometer (Tsuji *et al.*, 1998). The filled areas display the expected variations of the muon fluxes inside the angular bins $\Delta\theta = (26 - 34)^\circ$ (left panel) and $(69 - 81)^\circ$ (right panel). The solid curves are for the corresponding average zenith angles of 30° and 75°. The calculations presented in Fig. 8 are done without taking into account the geomagnetic effects (both the primary spectrum cutoff and muon deflection). These are not important under the conditions of Brookhaven and Kiel-DESY experiments but requisite for Okayama site.[10]

Generally the geomagnetic effects must decrease the low-momentum part of the expected muon flux (see top panel of Fig. 4). The calculated spectra fit rather well the precise Brookhaven and Kiel-DESY data but are in rather bad agreement (especially for $\theta = 30^\circ$) with the Okayama telescope data of poorer statistics; the geomagnetic corrections can only aggravate the disagreement. One can conclude from Fig. 8 that there is a systematic flaw in the average zenith angles measured in the Okayama experiment.

6 Numerical results for neutrinos

Let us briefly sketch some results on atmospheric neutrinos (AN). Due to geomagnetic effects, the low-energy AN spectra and angular distributions are quite different for different sites of the globe. Figures 9 and 10 display our predictions for ten underground neutrino laboratories listed in Table 1.

Figure 9 shows the ν_e, $\overline{\nu}_e$, ν_μ and $\overline{\nu}_\mu$ energy spectra averaged over all zenith and azimuth angles. The ratios of the AN fluxes averaged over the lower and upper semispheres ("up-to-down" ratios) are shown in Fig. 10. As a result of geomagnetic effects, both the spectra and the up-to-down ratios for the following 6 groups of the labs: SOUDAN + SNO + IMB, HPW, NUSEX + Fréjus, Gran Sasso + Baksan, Kamioka, and KGF are quite distinct for energies below a few GeV.

[10] The Okayama telescope location is $(34^\circ 40' \text{ N}, 133^\circ 56' \text{ E})$ and vertical geomagnetic cutoff rigidity is about 12.4 GV.

Table 1. List of some underground laboratories.

Lab/Detector	Country	Geographical location		Geomagnetic location		Token
SOUDAN	USA	48.00°N	92.00°W	58.32°	331.78°	• • •
SNO	Canada	46.80°N	82.00°W	57.90°	345.79°	- - - - -
IMB	USA	41.72°N	81.27°W	52.83°	346.30°	·····
HPW	USA	40.60°N	111.00°W	48.71°	311.28°	▲ ▲ ▲
NUSEX	Italy	45.86°N	6.90°E	47.24°	89.09°	▼ ▼ ▼
Fréjus	France	45.14°N	6.69°E	46.59°	88.59°	- · - · -
Gran Sasso	Italy	42.45°N	13.57°E	42.64°	94.27°	——
Baksan	Russia	43.30°N	42.70°E	38.06°	121.64°	★ ★ ★
Kamioka	Japan	36.42°N	137.31°E	26.19°	204.48°	□ □ □
KGF	India	3.00°N	78.30°E	3.25°	149.36°	■ ■ ■

Figure 11 depicts the zenith-angle distributions of ν_e, $\overline{\nu}_e$, ν_μ and $\overline{\nu}_\mu$ for Kamioka and Gran Sasso labs calculated with CORT using its "standard"(KM+SS) model of particle interaction (see sec. 4) and also the TARGET model for π/K meson production (including the superposition model for collisions of nuclei) used by Bartol group (Barr *et al.*, 1989; Agrawal *et al.*, 1996; Lipari *et al.*, 1998). The TARGET model for nucleon production is not included into the CORT options yet. Instead the KM+SS model is used everywhere. Below, we refer to CORT switched into the TARGET meson production model as "CORT+TARGET". For comparison, the result of the recent 3D calculation by Battistoni *et al.* (2000) based on the FLUKA 3D Monte Carlo simulation package is also shown. It allows to "highlight" the 3D effects which are very dependent on neutrino energy and direction of arrival.

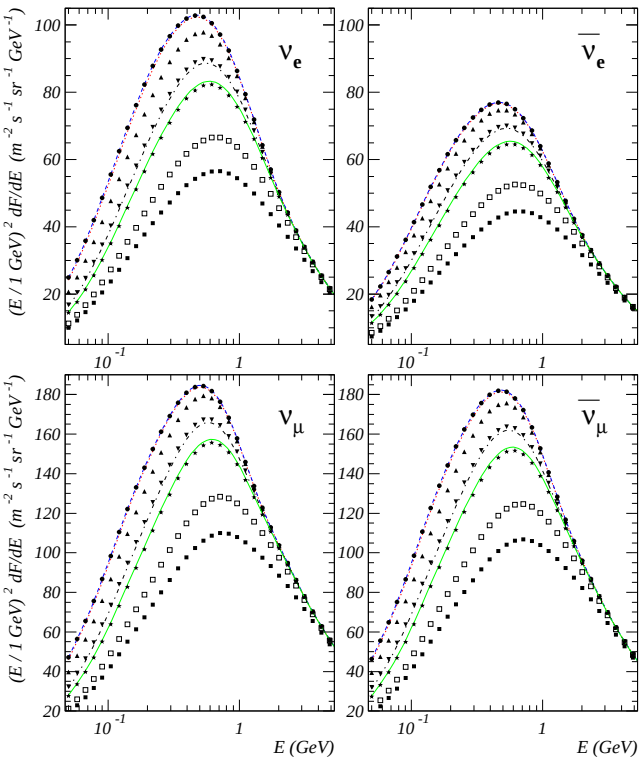

Fig. 9. Scaled 4π averaged fluxes of ν_e, $\overline{\nu}_e$, ν_μ, and $\overline{\nu}_\mu$ for ten underground laboratories (see table 1 for notation).

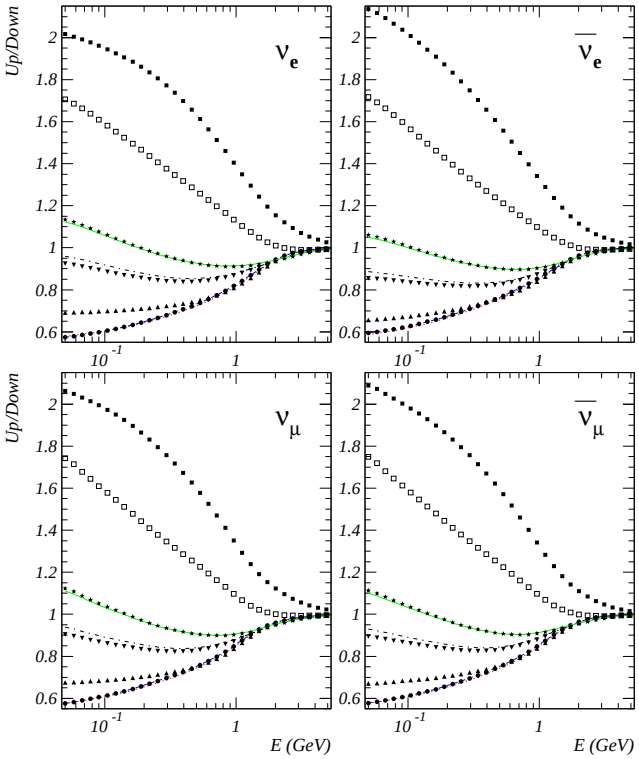

Fig. 10. Up-to-Down ratios of the ν_e, $\overline{\nu}_e$, ν_μ, and $\overline{\nu}_\mu$ fluxes for ten underground laboratories (see table 1 for notation).

A more quantitative comparison is given by Table 2 which tabulates the ratios of theν_e, $\overline{\nu}_e$, ν_μ, and $\overline{\nu}_\mu$ fluxes calculated with CORT+TARGET and FLUKA to those with the "standard" CORT. The fluxes are averaged over all directions and over several energy bins. Table 2 also shows the so-called flavor ratio[11]

$$R_\nu = \left(\nu_e + \tfrac{1}{3}\overline{\nu}_e\right) / \left(\nu_\mu + \tfrac{1}{3}\overline{\nu}_\mu\right),$$

evaluated with CORT, CORT+TARGET, and FLUKA for the same energy bins.

By using Fig. 11 and Table 2, one can conclude that the present calculations with CORT for neutrino energies below 1-2 GeV lead to the AN fluxes which are essentially *lower* than those obtained by Barr *et al.* (1989); Agrawal *et al.* (1996); Lipari *et al.* (1998) and by Honda *et al.* (1990, 1995, 1996) and those are in current use for many analyses of sub-GeV and multi-GeV ν induced events in underground detectors.[12] On the other hand, the new AN fluxes are rather close to the those obtained with the earlier versions of CORT (Bugaev and Naumov, 1987a,b, 1989, 1990). The main differences (for neutrino energies above 1-2 GeV) are due to the new data for the primary cosmic-ray spectrum and composition (see Section 3).

[11] This quantity roughly represents the ratio of e like to μ like single-ring contained events measured in water Cherenkov detectors and the "showers-to-tracks" ratio measured in iron detectors.

[12] A comparison between the earlier AN flux calculations has been discussed in detail by Gaisser *et al.* (1996).

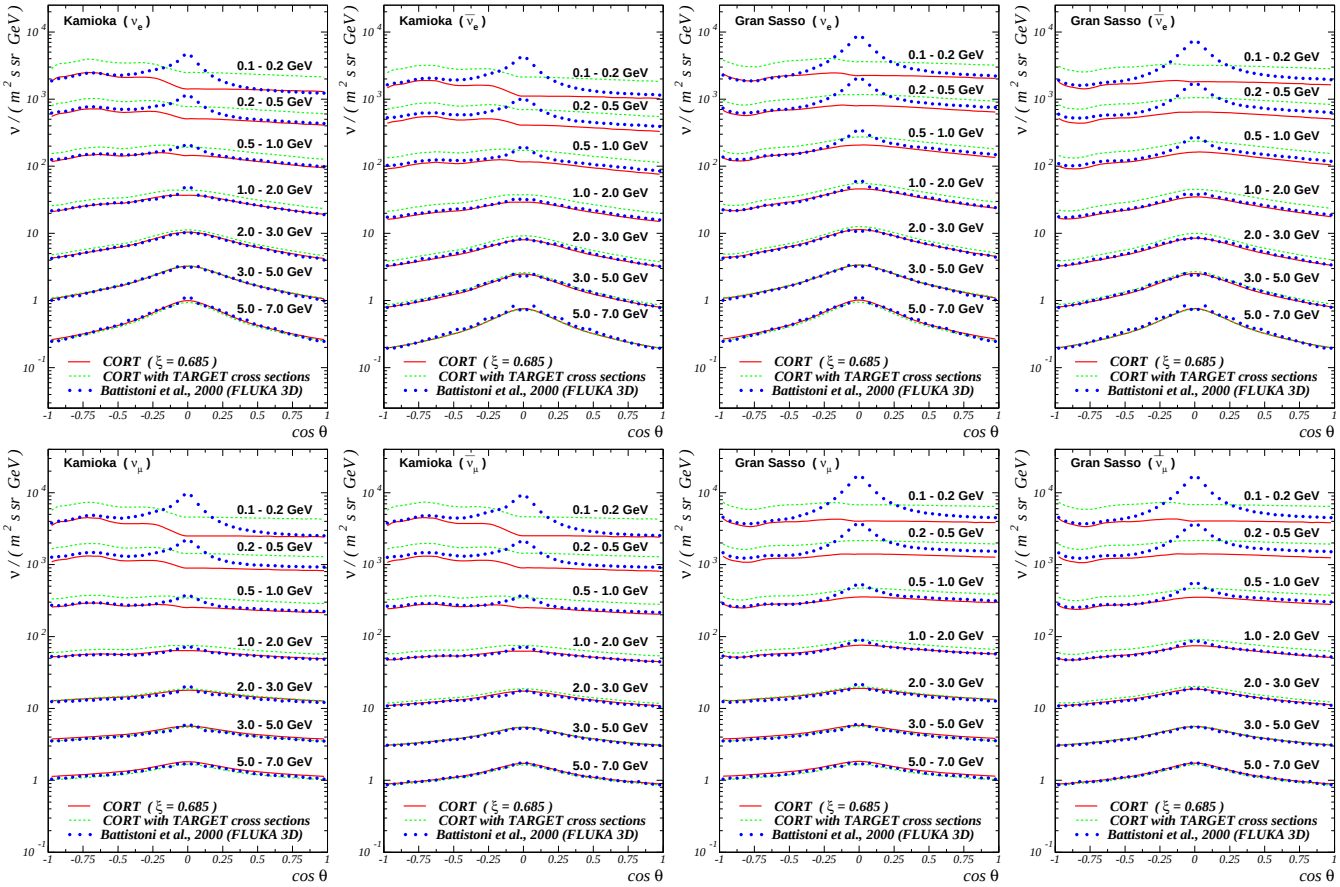

Fig. 11. Zenith-angle distributions of ν_e, $\overline{\nu}_e$, ν_μ, and $\overline{\nu}_\mu$ for Kamioka and Gran Sasso. Solid curves represent the result of CORT obtained with its "standard" interaction model. The dashed curves are the result of CORT obtained with the TARGET model for meson production and superposition model for collisions of nuclei. The circles are for the result of calculation by Battistoni *et al.* (2000) based on FLUKA 3D code. The distributions are averaged over the azimuth angle and over the energy bins indicated near the curves.

Table 2. The ratios of 4π averaged AN fluxes obtained with CORT+TARGET and FLUKA to those with CORT and neutrino flavor ratios R_ν calculated with CORT, CORT+TARGET, and FLUKA for Kamioka.

	Average fluxes normalized to CORT							
ΔE_ν	CORT+TARGET				FLUKA 3D			
(GeV)	ν_e	$\overline{\nu}_e$	ν_μ	$\overline{\nu}_\mu$	ν_e	$\overline{\nu}_e$	ν_μ	$\overline{\nu}_\mu$
0.1–0.2	1.64	1.78	1.72	1.73	1.25	1.45	1.41	1.40
0.2–0.3	1.51	1.68	1.60	1.61	1.23	1.38	1.34	1.33
0.3–0.5	1.42	1.61	1.48	1.50	1.17	1.28	1.22	1.22
0.5–0.7	1.34	1.50	1.36	1.38	1.10	1.19	1.11	1.12
0.7–1.0	1.28	1.41	1.27	1.30	1.05	1.12	1.04	1.05
1.0–2.0	1.20	1.30	1.17	1.20	1.02	1.05	0.99	1.01
2.0–3.0	1.10	1.17	1.03	1.08	0.98	1.03	0.96	0.97
3.0–5.0	1.02	1.07	0.95	1.01	0.99	1.02	0.95	0.97
5.0–7.0	0.95	0.99	0.91	0.96	1.01	1.05	0.94	0.99
7.0–10.0	0.91	0.95	0.89	0.93	1.03	1.09	0.95	1.04
10.0–20.0	0.87	0.91	0.88	0.91	1.07	1.12	0.96	1.02
20.0–30.0	0.83	0.87	0.87	0.89	1.10	1.15	0.94	1.02

	Flavor ratios R_ν		
ΔE_ν	CORT	CORT+TARGET	FLUKA 3D
(GeV)			
0.1–0.2	0.52	0.51	0.48
0.2–0.3	0.52	0.50	0.49
0.3–0.5	0.51	0.50	0.50
0.5–0.7	0.50	0.50	0.50
0.7–1.0	0.49	0.50	0.50
1.0–2.0	0.47	0.49	0.49
2.0–3.0	0.44	0.47	0.45
3.0–5.0	0.40	0.43	0.42
5.0–7.0	0.36	0.37	0.38
7.0–10.0	0.32	0.32	0.34
10.0–20.0	0.26	0.26	0.29
20.0–30.0	0.20	0.19	0.23

The AN angular distributions calculated with CORT and with FLUKA 3D code (Battistoni *et al.*, 2000, 2001b) are in good agreement for any zenith angle at energies above 0.7–0.8 GeV. On the other hand, CORT is systematically lower than FLUKA for $E_\nu \lesssim 1$ GeV. At the energy $E_\nu = 0.5$ GeV the FLUKA 4π averaged ν_e, $\overline{\nu}_e$, ν_μ and $\overline{\nu}_\mu$ fluxes exceed the corresponding CORT results by about 15%, 27%, 18% and 18%, respectively. This discrepancy is only partially due to 3D effects (Fig. 11), which can account for an increase $\lesssim 10\%$, and it is most probably related to differences between the hadronic interaction models adopted in FLUKA and CORT codes.

It is pertinent to note that several recent 3D Monte Carlo calculations of the AN flux (Honda *et al.*, 2001a,b; Liu *et al.*, 2001; Plyaskin, 2001; Tserkovnyak *et al.*, 2001; Wentz *et al.*, 2001a) confirmed the sharp enhancement of low-energy neutrino intensities for near-horizontal directions predicted with FLUKA. However the quantitative characteristics of this enhancement are very model-dependent and vary over a broad range from one calculation to another.

Prompt neutrinos

Figures 12 and 13 collect the differential energy spectra of downward going atmospheric neutrinos calculated within a wide energy range (from 50 MeV to about 20 EeV) for 11 zenith angles. Figures show the "conventional" neutrino contribution (originated from decay of pions, kaons and muons) and the total AN spectra which include the "prompt" neutrino contribution originated from semileptonic decays of charmed hadrons (mainly $D^\pm$, D^0, $\overline{D}^0$ mesons and Λ_c^+ hyperons).[13] The prompt neutrino contribution must dominate at very high energies. However the charm hadroproduction cross sections are very model-dependent and cannot be unambiguously predicted for lack of a generally accepted model. As a result the prompt neutrino contribution and even the energies above which the prompt muon and electron neutrinos become dominant are very uncertain as yet (Bugaev *et al.*, 1998; Pasquali *et al.*, 1998, 1999; Gelmini *et al.*, 2000a,b; Volkova & Zatsepin, 2001; Costa, 2001; Costa *et al.*, 2001). The results shown in Figs. 12 and 13 are obtained by using the two phenomenological approaches to the charm production problem: the quark-gluon string model (QGSM) and recombination quark-parton model (RQPM). The prompt muon fluxes predicted by QGSM and RQPM are both consistent with the current deep underground data and may be considered as the safe lower and upper limits for the prompt muon contributions. The basic assumptions of these models and the aspects of atmospheric cascade calculations were described by Bugaev *et al.* (1989).[14]

[13] We do not discuss here the contributions from D_s mesons and heavier states (such as $b\overline{b}$, $t\overline{t}$, W, Z) which become important sources of atmospheric (and extraterrestrial) prompt τ neutrinos at very high energies (Pasquali & Reno, 1999; Athar *et al.*, 2001).

[14] See also Refs. (Bugaev *et al.*, 1998; Naumov, 1998) for more details and related references.

Calculations of conventional AN fluxes for energies below ~ 100 GeV are done with CORT for Kamioka site, while the high-energy part of the conventional neutrino spectra as well as the prompt neutrino contributions are obtained by using the results of Ref. (Naumov *et al.*, 1998). Needless to say the high-energy AN fluxes are independent of location. The high-energy calculation takes into account many "thin" effects, like K_{e3} and $K_{\mu 3}$ form factors and K_S^0 semileptonic decays, meson regeneration and charge exchange through reactions $\pi^\pm + \mathrm{Air} \to \pi^{\pm(\mp)} + X$, $\pi^\pm + \mathrm{Air} \to K^{\pm(0)} + X$, etc., as well as through $K_{\pi 2}$ and $K_{\pi 3}$ decays. The low- and high-energy parts of the spectra are smoothly merged by using a polynomial (over $\log(E_\nu)$) clutching functions. The results of these calculations for all underground detectors are now embedded in a simple FORTRAN code "CORTout". It is based on a two-dimensional spline interpolation over the detailed tables and it may be useful for a fast evaluating the energy spectra and zenith-angle distributions of conventional and prompt atmospheric neutrinos within the energy range from 0.05 to $\sim 10^{10}$ GeV. The code is available upon request from the author.

7 Conclusions

Let us briefly re-state the main conclusions which follow from the outcome of Fiorentini *et al.* (2001a,b) and from the present study.

The results of extensive calculations performed with the new version of code CORT by using the updated KM+SS hadronic interaction model and the BESS+JACEE fit for the spectrum and composition of primary cosmic rays are in substantial agreement with a quite representative set of data on muon momentum spectra and charge ratios measured at different atmospheric depths, zenith angles, and geomagnetic locations. This provides a solid evidence for the validity of our description of hadronic interactions and shower development. The low-energy atmospheric neutrino fluxes calculated with CORT for many geomagnetic locations are systematically lower than those used in the current analyses of the data from underground neutrino experiments, while the neutrino flavor ratio and "up-to-down" asymmetry are essentially the same as in all recent calculations. It is difficult to increase the AN flux without spoiling the agreement with the current data on hadronic interactions, primary spectrum and muon fluxes.

Acknowledgements. It is pleasure to thank Gianni Fiorentini and Francesco Villante for their cooperation and for many constructive discussions. I thank Kostya Kuzmin and Segey Sinegovsky for significant contribution. I am thankful to Mirko Boezio, Patricia Hansen, Pierre Le Coultre, and Tomonori Wada for providing me with the data from CAPRICE 94/98, L3+C, and Okayama experiments before publication. I also thank Thomas Hebbeker and Charles Timmermans for their kind assistance in finding and understanding many experimental data. This research was supported in part by the Ministry of Education of the Russian Federation, the program "Universities of Russia" and by the Florence L3+C group.

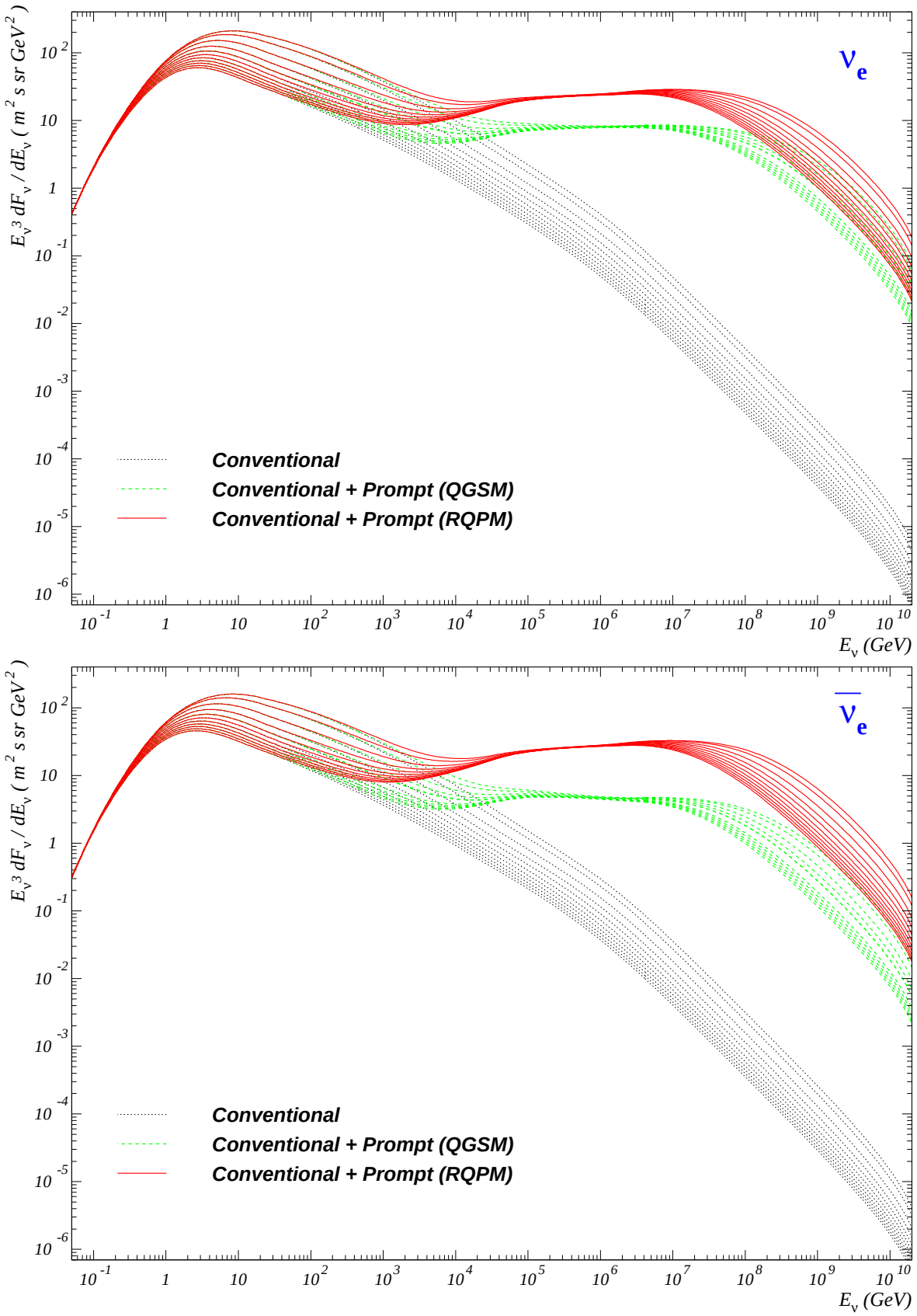

Fig. 12. Differential energy spectra of electron neutrinos and antineutrinos for 11 zenith angles θ. Low-energy range is for Kamioka site. Contributions from charm decay are calculated using recombination quark-parton model (RQPM) and quark-gluon string model (QGSM). At high energies, from smallest to largest fluxes, $\cos\theta$ varies from 0 to 1 with an increment of 0.1 for each group of curves.

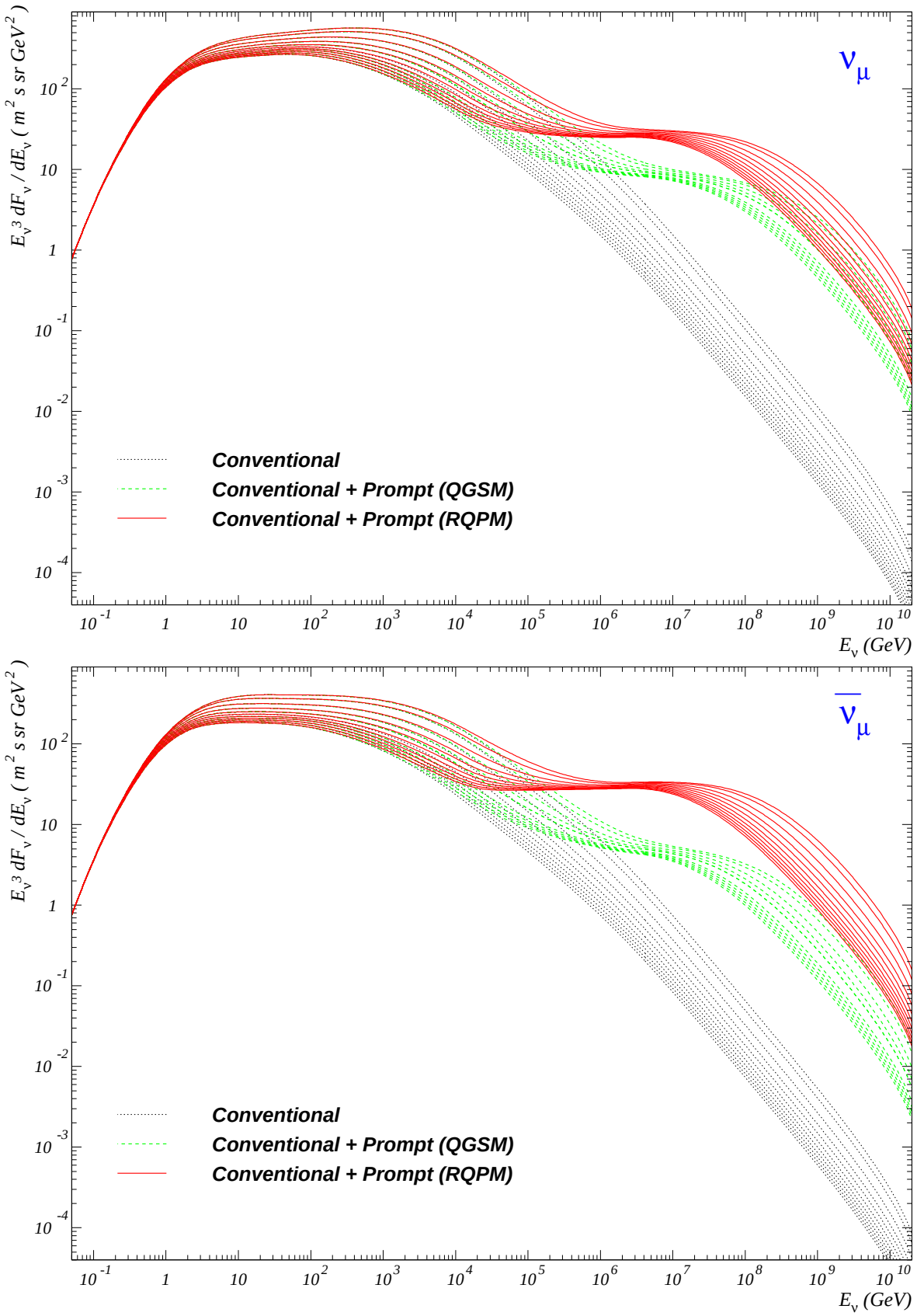

Fig. 13. Differential energy spectra of muon neutrinos and antineutrinos for 11 zenith angles θ. Low-energy range is for Kamioka site. Contributions from charm decay are calculated using recombination quark-parton model (RQPM) and quark-gluon string model (QGSM). At high energies, from smallest to largest fluxes, $\cos\theta$ varies from 0 to 1 with an increment of 0.1 for each group of curves.

References

Abdel-Monem, M.S. *et al.*, in: Proc. of the 13th Intern. Cosmic Ray Conf., Denver, 1973, Vol. **3**, p. 1811.

Agrawal, V. *et al.*, Phys. Rev. D **53**, 1314, 1996.

Aharonian, F. *et al.*, Phys. Rev. D **59**, 092003, 1999.

Alcaraz, J. *et al.* Phys. Lett. B **472**, 215, 2000.

Alcaraz, J. *et al.* Phys. Lett. B **490**, 27, 2000.

Alcaraz, J. *et al.* Phys. Lett. B **494**, 193, 2000.

Allkofer, O.C., Andresen, R.D., and Dau, W.D., Can. J. Phys. **46**, S301, 1968.

Allkofer, O.C. and Clausen, K., Acta. Phys. Acad. Sci. Hung. **29** (Suppl. 2), 698, 1970.

Allkofer, O.C., Dau, W.D., and Jokisch, H., Phys. Lett. **31** B, 606, 1970; *ibid.*, **36** B, 428, 1971 (Erratum).

Allkofer, O.C., Carstensen, K., and Dau, W.D., Phys. Lett. **36** B, 425, 1971.

Allkofer, O.C. and Dau, W.D., Phys. Lett. **38** B, 439, 1972.

Allkofer, O.C., Clausen, K., and Dau, W.D., Lett. Nuovo Cim. **12**, 107, 1975.

Appleton, I.C., Hogue, M.T., and Rastin, B.C., Nucl. Phys. B **26**, 365, 1971.

Asakimori, K. *et al.*, Astrophys. J. **502**, 278, 1998.

Athar, H. *et al.*, hep–ph/0112222.

Aurela, A.M. and Wolfendale, A.W., Annales Acad. Sci. Fenn. A **6**, Vol. **227**, 1, 1967.

Ayre, C.A. *et al.*, in: Proc. of the 13th Intern. Cosmic Ray Conf., Denver, 1973, Vol. **3**, p. 1822.

Ayre, C.A. *et al.*, J. Phys. G: Nucl. Phys. **1**, 584, 1975.

Baber, S.R., Nash, W.F., and Rastin, B.C., Nucl. Phys. B **4**, 539, 1968.

Baber, S.R., Nash, W.F., and Rastin, B.C., Nucl. Phys. B **4**, 549, 1968.

Barr, G., Gaisser, T.K., and Stanev, T., Phys. Rev. D **39**, 3532, 1989.

Baschiera, B. *et al.*, Nuovo Cim. C **2**, 473, 1979.

Bateman, B.J. *et al.*, Phys. Lett. **36** B, 144, 1971.

Battistoni, G. *et al.*, Astropart. Phys. **12**, 315, 2000. For the current FLUKA results see URL http://www.mi.infn.it/~battist/neutrino.html.

Battistoni, G. *et al.*, hep–ph/0107241

Battistoni, G. *et al.*, hep-ph/0112072.

Baxendale, J.M., Hume, C.J., and Thompson, M.G., J. Phys. G: Nucl. Phys. **1**, 781, 1975.

Beatty, J.J. *et al.*, Astrophys. J. **413**, 268, 1993.

Bellotti, R. *et al.*, Phys. Rev. D **60**, 052002, 1999.

Bialas, A., Bleszyński, M., and Czyż, W., Nucl. Phys. B **111**, 461, 1976.

Boezio, M. *et al.*, Astrophys. J. **518**, 457, 1999.

Boezio, M. *et al.*, Phys. Rev. Lett. **82**, 4757, 1999.

Boezio, M. *et al.*, Phys. Rev. D **62**, 032007, 2000; Boesio, M., private communication (September, 2001).

Brancus, I.M. *et al.*, Acta Phys. Polon. B **31**, 465, 2000.

Buckley, J. *et al.*, Astrophys. J. **429**, 736, 1994.

Bugaev, E.V. and Naumov, V.A., Investigations on Geomagnetism, Aeronomy and Solar Physics, **73**, 198, 1984.

Bugaev, E.V. and Naumov, V.A., Inst. for Nuclear Research, USSR Acad. of Sci., Reports II–0385 and II–0401, Moscow, 1985.

Bugaev, E.V. and Naumov, V.A., Izv. Akad. Nauk SSSR, Ser. Fiz. **50**, 2239, 1986 [Bull. Russ. Acad. Sci. Phys. **50, N. 11**, 156, 1986].

Bugaev, E.V. and Naumov, V.A., Yad. Fiz. **45**, 1380, 1987 [Sov. J. Nucl. Phys. **45**, 857, 1987].

Bugaev, E.V. and Naumov, V.A., Inst. for Nuclear Research, USSR Acad. of Sci., Report II-0537, Moscow, 1987.

Bugaev, E.V. and Naumov, V.A., in: Proc. of the 2nd Intern. Symposium "Underground Physics'87", Baksan Valley, 1987, ed. by Domogatsky, G.V. *et al.* (Moscow, "Nauka", 1988) p. 255.

Bugaev, E.V. and Naumov, V.A., Phys. Lett. B **232**, 391, 1989.

Bugaev, E.V. *et al.*, Nuovo Cim. C. **12**, 41, 1989.

Bugaev, E.V. and Naumov, V.A., Yad. Fiz. **51**, 774, 1990 [Sov. J. Nucl. Phys. **51**, 493, 1990].

Bugaev, E.V. *et al.*, Phys. Rev. D **58**, 054001, 1998 (see also hep–ph/9803488 for more details).

Burnett, T.H. *et al.*, Phys. Rev. Lett. **30**, 937, 1973.

Caro, D.E., Parry, J.K., and Rathgeber, H.D., Nature **165**, 689, 1950.

Coates, D.W. and Nash, W.F., Austral. J. Phys. **15**, 420, 1962.

Conversi, M., Phys. Rev. **79**, 749, 1950.

Costa, C.G.S., Astropart. Phys. **16**, 193, 2001.

Costa, C.G.S., Halzen, F., and Salles, C., hep–ph/0104039.

Coutu, S. *et al.*, Phys. Rev. D **62**, 032001, 2000.

Diehl, E. *et al.*, in: Proc. of the 25th Intern. Cosmic Ray Conf., Durban, 1997, Vol. **3**, pp. 405. No result presented in this paper. The data are taken from von Rosenvinge, T.T. *ibid.*, Vol. **8**, p.237.

Dorman, L.I., Smirnov, V.S., and Tiasto, M.I., *Cosmic rays in the magnetic field of the Earth*, "Nauka", Moscow, 1971.

Dorman, L.I., *Meteorological effects of cosmic rays*, "Nauka", Moscow, 1972.

Engel, R., Gaisser, T.K., and Stanev, T., in: Proc. of the 27th Intern. Cosmic Ray Conf., Hamburg, 2001, Vol. **3**, p. 1029.

Filosofo, I., Pohl, E., and Pohl-Rüling, J., Nuovo Cim. **12**, 809, 1954.

Fiorentini, G., Naumov, V.A., and Villante, F.L., Phys. Lett. B **510**, 173, 2001.

Fiorentini, G., Naumov, V.A., and Villante, F.L., in: Proc. of the 27th Intern. Cosmic Ray Conf., Hamburg, 2001, Vol. **3**, p. 1218 (hep–ph/0106014).

Fukui, S., J. Phys. Soc. Jap. **10**, 735, 1955.

Gaisser, T.K. *et al.*, Phys. Rev. D **54**, 5578, 1996.

Gelmini, G., Gondolo, P., and Varieschi, G., Phys. Rev. D **61**, 036005, 2000.

Gelmini, G., Gondolo, P., and Varieschi, G., Phys. Rev. D **61**, 056011, 2000.

Grandegger, W., KfK Report 5122, Kernforschungszentrum Karlsruhe, 1993.

Green, P.J. *et al.*, Phys. Rev. D **20**, 1598, 1979.

Grieder, P.K.F., *Cosmic rays at Earth*, North-Holland, Elsevier Science Publishers B. V., Amsterdam, 2001.

Hansen, P. *et al.*, in: Proc. of the 27th Intern. Cosmic Ray Conf., Hamburg, 2001, Vol. **1**, p. 921; Hansen, P., private communication (September, 2001).

Hayman, P.J. and Wolfendale, A.W., Proc. Phys. Soc. (London) A **80**, 710, 1962.

Hayman, P.J. and Wolfendale, A.W., Nature **195**, 166, 1962.

Hebbeker, T. and Timmermans, C., hep–ph/0102042 (submitted to Astropart. Phys.).

Holmes, J.E.R., Owen, B.G., and Rodgers, A.L., Proc. Phys. Soc. (London) A **78**, 505, 1961.

Honda, M. *et al.*, Phys. Lett. B **248**, 193, 1990.

Honda, M. *et al.*, Phys. Rev. D **52**, 4985, 1995.

Honda, M. *et al.*, Prog. Theor. Phys. Suppl. **123**, 483, 1996.

Honda, M. *et al.*, Phys. Rev. D **64**, 053011, 2001.

Honda, M. *et al.*, in: Proc. of the 27th Intern. Cosmic Ray Conf., Hamburg, 2001, Vol. **3**, p. 1162.

Ichimura, M. *et al.*, Phys. Rev. D **48**, 1949, 1993.

Jannakos, T.E., FZKA Report 5520, Forschungszentrum Karlsruhe, 1995.

Jokisch, H. *et al.* Phys. Rev. D **19**, 1368, 1979.

Kalinovsky, A.N., Mokhov, N.V., and Nikitin, Yu.P., *Transport of high-energy particles through matter*, "Energoatomizdat", Moscow, 1985.

Kawaguchi, S. *et al.*, in: Proc. of the 9th Intern. Cosmic Ray Conf., London, 1965, Vol. **2**, p. 941.

Kellogg, R.G., Kasha, H., and Larsen, R.C., Phys. Rev. D **17**, 98, 1978.

Kimel', L.R. and Mokhov, N.V., Izv. Vuz. Fiz. **10**, 17, 1974.

Kimel', L.R. and Mokhov, N.V., Problems of Dosimetry and Radiation Protection, **14**, 41, 1975.

Kowalski, M. and Bartke, J., Acta Phys. Polon. B **12**, 759, 1981.

Kremer, J. *et al.*, Phys. Rev. Lett. **83**, 4241, 1999.

Krizmanic, J.F. *et al.*, in: Proc. of the 24th Intern. Cosmic Ray Conf., Rome, 1995, Vol. **1**, p. 593.

Ladron de Guevara, P. (for the L3 Collaboration), Nucl. Phys. B (Proc. Suppl.) **95**, 237, 2001.

Le Coultre, P. (for the L3+C Collaboration), in: Proc. of the 27th Intern. Cosmic Ray Conf., Hamburg, 2001, Vol. **3**, p. 974; Le Coultre, P., private communication (August, 2001)

Lipari, P., Gaisser, T.K., and Stanev, T., Phys. Rev. D **58**, 073003, 1998.

Liu, Y., Derome, L., and Buénerd, M., in: Proc. of the 27th Intern. Cosmic Ray Conf., Hamburg, 2001, Vol. **3**, p. 1033.

Mason, G.M., Astrophys. J. **171**, 139, 1972.

Menn, W. *et al.*, Astrophys. J. **533**, 281, 2000.

Moroney, J.R. and Parry, J.K., Austral. J. Phys. **7**, 424, 1954.

Motoki, M. *et al.*, in: Proc. of the 27th Intern. Cosmic Ray Conf., Hamburg, 2001, Vol. **1**, p. 927.

Nandi, B.C. and Sinha, M.S., J. Phys. A: Gen. Phys. **5**, 1384, 1972.

Nandi, B.C. and Sinha, M.S., Nucl. Phys. B **40**, 289, 1972.

Naumov, V.A., Investigations on Geomagnetism, Aeronomy and Solar Physics, **69**, 82, 1984.

Naumov, V.A., in: Proc. of the Intern. Workshop on ν_μ/ν_e Problem in Atmospheric Neutrinos, Gran Sasso, 1993, eds. Berezinsky, V.S. and Fiorentini, G. (LNGS, L'Aquila, 1993), p. 25.

Naumov, V.A., in: Proc. the Baikal School on Fundamental Physics "Astrophysics and Microworld Physics", Irkutsk, 1998, eds. Naumov, V.A., Parfenov, Yu.V, and Sinegovsky, S.I., (Irkutsk State University, Irkutsk, 1998), p. 67.

Naumov, V.A., *Atmospheric muons and neutrinos*, see URL of this Workshop, Program and Transparencies (Talks and Posters): http://www-zeuthen.desy.de/nuastro/publications/sources/workshop2001/icpost_tr.html.

Naumov, V.A. and Sinegovskaya, T.S., Yad. Fiz. **63**, 2020, 2000 [Phys. Atom. Nucl. **63**, 1927, 2000].

Naumov, V.A. and Sinegovskaya, T.S., in: Proc. of the 27th Intern. Cosmic Ray Conf., Hamburg, 2001, Vol. **1**, p. 4173 (hep–ph/0106015).

Naumov, V.A., Sinegovskaya, T.S., and Sinegovsky, S.I., Nuovo Cim. A **111**, 129, 1998.

Naumov, V.A., Sinegovskaya, T.S., and Sinegovsky, S.I., Yad. Fiz. **63**, 2016, 2000 [Phys. Atom. Nucl. **63**, 1923, 2000].

Naumov, V.A., Sinegovsky, S.I., and Bugaev, E.V., Yad. Fiz. **57**, 439, 1994 [Phys. Atom. Nucl. **57**, 412, 1994]; hep–ph/9301263.

Owen, B.G. and Wilson, J.G., Proc. Phys. Soc. (London) A **62**, 601, 1949.

Owen, B.G. and Wilson, J.G., Proc. Phys. Soc. (London) A **64**, 417, 1951.

Owen, B.G. and Wilson, J.G., Proc. Phys. Soc. (London) A **68**, 409, 1955.

Pak, W. *et al.*, Phys. Rev. **121**, 905, 1961.

Pasquali, L., Reno, M.H., and Sarcevic, I., Astropart. Phys. **9**, 193, 1998.

Pasquali, L., Reno, M.H., and Sarcevic, I., Phys. Rev. D **59**, 034020, 1999.

Pasquali, L. and Reno, M.H., Phys. Rev. D **59**, 093003, 1999.

Petersen, B. (for the L3 Collaboration), Nuovo Cim. C **24**, 751, 2001.

Pine, J., Davidson, R.J., and Greisen, K., Nuovo Cim. **14**, 1181, 1959.

Plyaskin, V., Phys. Lett. B **516**, 213, 2001.

Poirier, J., Roesler, S., and Fasso, A., astro–ph/0103030 (also SLAC-PUB-8945).

Rastin, B.C. *et al.*, in: Proc. of the 9th Intern. Cosmic Ray Conf., London, 1965, Vol. **2**, p. 981.

Rastin, B.C., J. Phys G: Nucl. Phys. **10**, 1609, 1984.

Rastin, B.C., J. Phys G: Nucl. Phys. **10**, 1629, 1984.

Ryan, M.J., Ormes, J.F., and Balasubrahmanyan, V.K., Phys. Rev. Lett. **28**, 985, 1972; *ibid.* **28**, 1497, 1972 (Erratum).

Sanuki, T. *et al.*, Astrophys. J. **545**, 1135, 2000.

Sanuki, T. (for the BESS collaboration), Nucl. Phys. B (Proc. Suppl.) **100**, 121, 2001.

Sanuki, T. *et al.*, in: Proc. of the 27th Intern. Cosmic Ray Conf., Hamburg, 2001, Vol. **1**, p. 950.

Seo, E.S. *et al.*, Astrophys. J. **378**, 763, 1991.

Serov, A.Ya. and Sychev, B.S., Transactions of the Moscow Radio-Engineering Institute, **11**, 173, 1973.

Sinegovskaya, T.S. and Sinegovsky, S.I., Phys. Rev. D **63**, 096004, 2001.

Singhal, K.P., in: Proc. of the 18th Intern. Cosmic Ray Conf., Bangalore, 1983, Vol. **7**, p. 27.

Smart, D.F. and Shea, M.A., Adv. Space Res. **14**, 787, 1994.

Stephens, S.A. and Golden, R.L., in: Proc. of the 20th Intern. Cosmic Ray Conf., Moscow, 1987, Vol. **6**, p. 173.

Sychev, B.S., *Cross sections for interactions of high-energy hadrons with atomic nuclei*, Moscow Radio-Engineering Inst. of the Russian Acad. of Sci., Moscow, 1999.

Thompson, M.G. *et al.*, in: Proc. of the 15th Intern. Cosmic Ray Conf., Plovdiv, 1977, Vol. **6**, p. 21.

Tserkovnyak, Y. *et al.*, in: Proc. of the 27th Intern. Cosmic Ray Conf., Hamburg, 2001, Vol. **3**, p. 1196.

Tsuji, S. *et al.*, J. Phys. G: Nucl. Part. Phys. **24**, 1805, 1998.

Tsuji, S. *et al.*, in: Proc. of the 27th Intern. Cosmic Ray Conf., Hamburg, 2001, Vol. **3**, p. 935; Wada, T., private communication (July, 2001).

Vall, A.N., Naumov, V.A., and Sinegovsky, S.I., Yad. Fiz. **44**, 1240, 1986 [Sov. J. Nucl. Phys. **44**, 806, 1986].

Volkova, L.V and Zatsepin, G.T., Yad. Fiz. **64**, 313, 2001 [Phys. Atom. Nucl. **64**, 266, 2001].

Vulpescu, B. *et al.*, Nucl. Instr. Meth. A **414**, 205, 1998.

Vulpescu, B. *et al.*, J. Phys. G **27**, 977, 2001.

Wentz, J. *et al.*, in: Proc. of the 27th Intern. Cosmic Ray Conf., Hamburg, 2001, Vol. **3**, p. 1167.

Wentz, J. *et al.*, J. Phys. G **27**, 1699, 2001.

Wiebel-Sooth, B., Biermann, P.L., and Meyer, H., Astron. Astrophys. **330**, 389, 1998.